Aggregation properties of amphiphilic DNA-carriers for gene delivery

Scarzello, Marco

CHAPTER 2

POLYMORPHISM OF SAINT AMPHIPHILES: INFLUENCE OF IONIC STRENGTH, HELPER LIPID CONTENT AND PLASMID-DNA COMPLEXATION

Two double-tailed pyridinium cationic amphiphiles, differing only in the degree of unsaturation of the alkyl chains, have been selected for a detailed study of their aggregation behavior, under conditions employed for transfection experiments. The transfection efficiencies of the two molecules are remarkably different, especially when combined with DOPE as helper lipid. The phase behavior of the cationic amphiphile/DOPE mixtures has been studied, using ^{31}P- and ^{2}H-NMR (on deuterated cationic amphiphiles) as main techniques, in order to monitor independently the behavior of the two components. In water, the lamellar organization is dominant for both surfactants in their mixtures with the helper lipid. In HBS (Hepes saline buffer), the mixtures of the unsaturated surfactant form inverted phases and, in particular, stable H_{II} phases for DOPE contents equal or higher than 30 mol%. By contrast, the saturated surfactant does not form homogeneously mixed inverted phases in mixtures with DOPE at room temperature. However, mixed inverted phases are observed for this system at higher temperatures and, after mixing has been achieved by heating, the metastable mixed phases remain present for several hours at 5ºC. At 35ºC the dominant phase is the cubic phase. The lipoplex composed of equimolar mixtures of the unsaturated surfactant with DOPE and plasmid DNA was found to be organized in highly curved bilayers.

In Appendix 1, the results of a preliminary study of the phase behavior of SAINT-2 in water, at high lipid concentrations, are presented.

Part of this chapter has been published: Scarzello, M.; Chupin, V.; Wagenaar, A.; Stuart, M. C. A.; Engberts, J. B. F. N.; Hulst, R. *Biophys. J.* **2005,** *88*, 2104-2113.

2.1 INTRODUCTION

This study was focused on the polymorphism of two well-studied SAINT amphiphiles (Paragraph 1.4.1), SAINT-2 and SAINT-5 (Figure 1), differing only in the degree of unsaturation of the alkyl chains, $C_{18:1}$ and $C_{18:0}$, respectively. The aggregation properties of the two selected pyridinium amphiphiles in mixtures with the zwitterionic phospholipid DOPE have been determined under conditions as employed in transfection experiments.

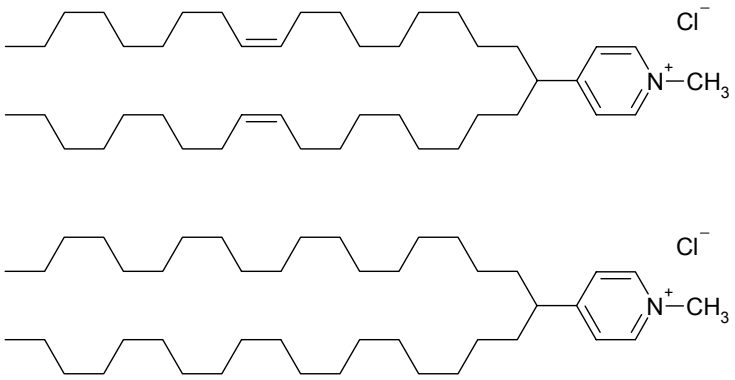

Figure 1 *SAINT-2 (top) and SAINT-5 (bottom) cationic amphiphiles.*

A previous comparative study on SAINT-2 and SAINT-5 revealed that simple structural modifications as the degree of unsaturation of the alkyl chains give rise to dramatic differences in the transfection potential.[1] The differences in behavior between the two molecules become even more pronounced when a helper lipid is added to the transfection cocktail: while DOPE strongly promotes SAINT-2-mediated transfection, SAINT-5-mediated transfection remains virtually unaffected upon addition of DOPE. The results have been rationalized in terms of tighter packing of the saturated chains of SAINT-5 in the bilayer in comparison with the unsaturated chains of SAINT-2, resulting in a higher stiffness of the membrane formed by SAINT-5. The interaction of DNA with a poorly deformable cationic membrane leads to a less favourable lipoplex assembly, inefficient DNA translocation and, consequently, to a low(er) transfection efficiency.[1]

In the present study, we have investigated the physico-chemical differences between SAINT-2 and SAINT-5, as revealed by ^{2}H-NMR, ^{31}P-NMR and cryo-TEM. The advantages of this approach arise from the possibility of carrying out experiments under conditions which are close to those of transfection experiments and in the complete absence of perturbative probes.

^{2}H-NMR has been previously used to examine the effect of the complexation of polyadenilic acid on mixtures of cationic amphiphiles and phospholipids[2] and ^{31}P-NMR has been used to monitor the morphology of the DOTMA lipoplex with plasmid DNA.[3] This powerful combination of ^{31}P- and ^{2}H-NMR techniques has, however, not previously been employed to study transfection cocktails. Monitoring independently the phase behavior of the cationic amphiphiles (^{2}H-NMR) and helper lipid (^{31}P-NMR) in these mixtures, before and after complexation with DNA, yields important insights into the extent of mixing of the two lipid components. The effects of ionic strength, temperature (cycles) and different amounts of helper lipid on the phase behavior of the two pyridinium amphiphiles have also been determined. Finally, the consequences of plasmid-DNA binding for the properties of the aggregate are examined for the lipoplex with the highest transfection efficiency, *i.e.* the complex between the equimolar mixture of SAINT-2/DOPE with DNA at a charge ratio +/- = 2.5.

2.2 SYNTHESIS OF DEUTERATED SAINT AMPHIPHILES

As mentioned in Chapter 1, one of the common attractive features of the three classes of cationic amphiphiles under study is that the synthetic protocols allow the easy introduction of structural modifications to the basic framework. The synthesis of the SAINTs[4,5] is shown in Scheme 1.

Scheme 1 *Basic synthetic protocol for the preparation of the SAINT amphiphiles.*

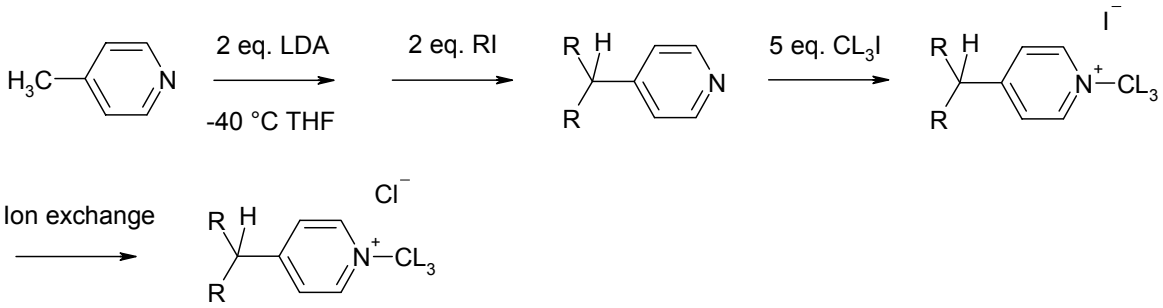

L indicates ^{1}H or ^{2}H atoms.

Starting from 4-picoline, a bis-deprotonation with LDA followed by a double alkylation with the appropriate alkyl iodide yields the substituted pyridine. The quaternization of the pyridine nitrogen is simply performed by reaction with an excess of methyl iodide. The final step consists of an ion exchange on a Sephadex column which provides the chloride salt of

the cationic amphiphile. The deuterated SAINT amphiphiles used in the ^{2}H-NMR experiments (*vide infra*) were obtained using deuterated starting materials (*i.e.* methyl iodide-d_3).

2.3 MIXTURES OF SAINT-2 AND DOPE

2.3.1 Phase Behavior in Water

The phase behavior of mixtures of the cationic amphiphiles with DOPE has been studied combining ^{31}P-NMR and ^{2}H-NMR (of the N-methyl deuterated SAINTs) in order to monitor independently the properties of both components in the mixture.

The ^{31}P-NMR spectra of equimolar mixtures of SAINT-2/DOPE in water at different temperatures are shown in Figure 2 (top row). The spectrum at 5°C consists of a superposition of a signal characterized by an high field peak and a low field shoulder, indicating the presence of an L_α phase[6] (chemical shift anisotropy, CSA = + 54 ppm), and a symmetric peak centred at 0 ppm (isotropic peak), of which the contribution increases with temperature. The large value of the CSA measured for the L_α phase compared to that of pure phospholipids is explained by the conformational changes of the headgroups induced by the presence of the cationic amphiphile.[7]

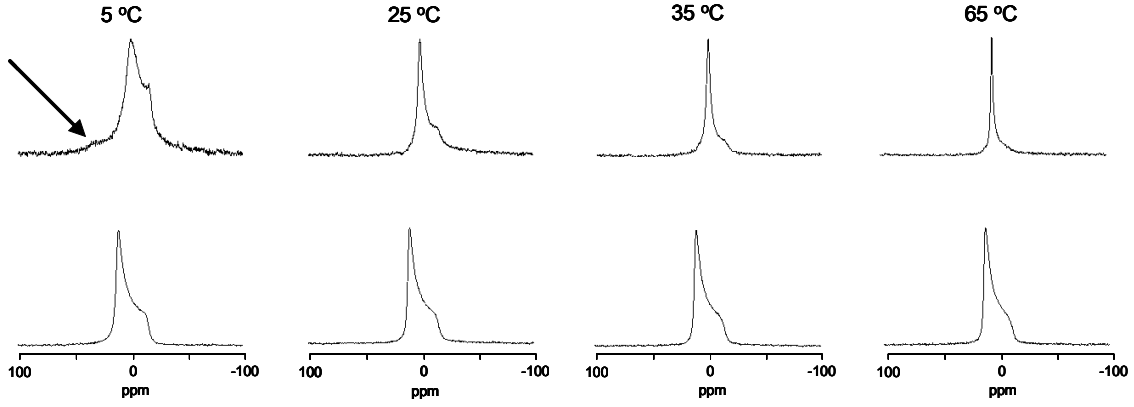

Figure 2 *^{31}P-NMR spectra as a function of increasing temperature of samples of SAINT-2 mixed with DOPE (1/1 molar ratio, 100 mM total lipid concentration) in water (top row) and in HBS (bottom row). The arrow indicates the low field shoulder.*

As described in Paragraph 1.6.1.1, the averaging of the CSA leading to the isotropic peak can be due to the tumbling of small aggregates, lateral diffusion around small diameter particles or by the organization of the lipids in an isotropic phase (*e.g.* a cubic phase).[6]

The homogeneous appearance of the samples upon visual inspection and previous SAXS results, which revealed that the pelleted vesicles maintain a lamellar morphology, suggest that the isotropic peak observed in water results from lipids in a bilayer organization as characterized by short correlation times and not from the transition towards an inverted isotropic phase; this conclusion is consistent with the reversibility of the line shape variations observed monitoring the cooling behavior, also for short equilibration times (< 30 min).

2.3.2 Phase Behavior at Physiological Ionic Strength: Transition towards an H_{II} Phase

Increasing the ionic strength of the solution to physiological values has a dramatic effect on the phase behavior of the system, as indicated by the ^{31}P-NMR line shapes (Figure 2, bottom row), which are now characterized by a low field peak and an high field shoulder, with a span of the anisotropy (CSA= -27 ppm) equal to half the one observed for the lamellar phase. The inversion of the asymmetry and the reduction of the CSA upon going from water to HBS indicate a transition from the L_α phase to the H_{II} phase.[6] The spectra indicate a quantitative conversion to the H_{II} phase, since signals arising from L_α phases are no longer detectable. The remarkable thermal stability of the H_{II} phase is indicated by the absence of significant variations in the line shapes in the whole range of temperatures explored.

In order to determine the behavior of the SAINT amphiphile in the mixture independently, ^{2}H-NMR spectra have been recorded on samples consisting of DOPE and deuterated cationic lipid (Figure 3). Since pure DOPE in water forms an H_{II} phase at temperatures higher than 10°C, while SAINT-2 assumes a lamellar morphology,[8] the ^{2}H-NMR experiments allowed to verify whether the phases observed with ^{31}P-NMR arise from homogeneous mixtures of the two lipid components or from domains of unmixed DOPE. In the presence of an equimolar amount of DOPE, the cationic amphiphile produces in water a Pake pattern line shape[9] with a quadrupolar splitting, $\Delta\nu_Q$ = 18 KHz (see Paragraph 1.6.1.2), superimposed on a broad isotropic peak. Also the spectra of the samples in HBS present a well-resolved Pake pattern, with a quadrupolar splitting of $\Delta\nu_Q$ = 9.8 KHz, about half the quadrupolar splitting observed for the same sample in water, together with a very sharp isotropic peak, which can be assigned to the deuterium naturally present in water. For the samples in water, the ^{2}H-NMR line shapes are consistent with aggregates of different dimensions in the L_α phase. The reduction of the quadrupolar splitting upon going from water to HBS confirms the quantitative conversion to the H_{II} phase. The absence of significant variations in the line

shape of the ^{2}H-NMR spectra recorded in HBS as a function of temperature confirms the stability of the H_{II} assembly, as already deduced from the ^{31}P-NMR spectra.

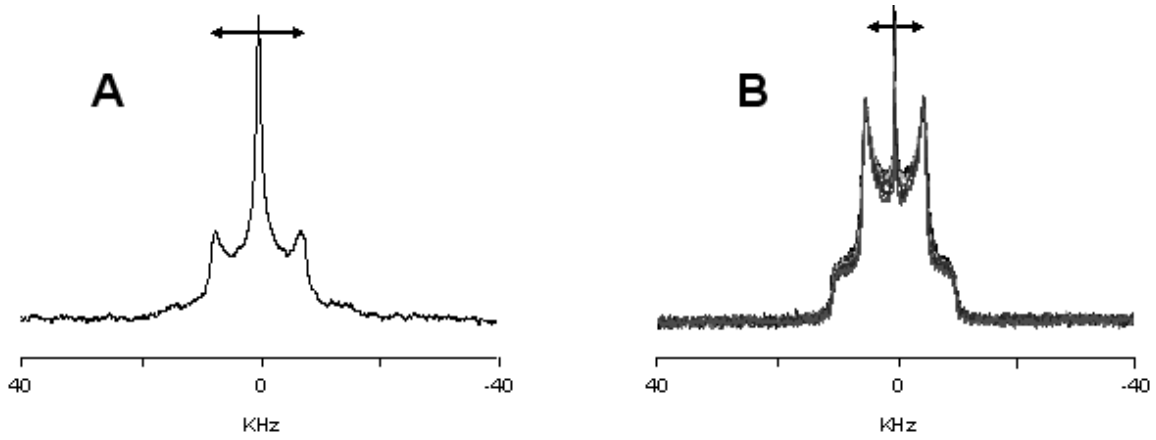

Figure 3 *^{2}H-NMR spectra of samples of SAINT-2 deuterated at the N-methyl mixed with DOPE (1/1 molar ratio, 100 mM total lipid concentration) in water at 25°C (A) and in HBS (B) at 25, 35, 40, 45, 55, 60, 65 °C. Arrows indicate the quadrupolar splittings.*

^{31}P- and ^{2}H-NMR spectra of the SAINT-2/DOPE mixture in HBS show that DOPE and SAINT-2 are present in an H_{II} phase and that the line shapes of both the ^{2}H- and ^{31}P-NMR spectra reveal the same temperature independence: the CSA of ^{31}P and the $\Delta\nu_Q$ of ^{2}H remain constant between 25 and 65 °C. These observations, together with the fact that the lipoplex of SAINT-2 in the absence of DOPE at physiological ionic strength exhibits a lamellar morphology,[8] represent a strong indication for the homogeneous mixing of the unsaturated cationic amphiphile with DOPE.

The effect of pH variations has been determined by comparing the spectra of the suspensions in HBS with those performed on samples hydrated with an aqueous solution containing 150 mM of NaCl. The perfect correspondence between the line shapes in the two media indicates that the degree of protonation of the headgroup of DOPE does not change significantly upon the variation in pH and that the quantitative transition toward the H_{II} phase is induced by the increase in ionic strength. The main consequence of the presence of physiological concentrations of aqueous NaCl is the screening of the electrostatic repulsion between the headgroups of the cationic amphiphile. This effect leads to a decrease of a_0 (see Paragraph 1.2.2) and, consequently, to an increase of the packing parameter P, consistent with the transition to the inverted phase.

Decreasing the amount of DOPE decreases the average P of the mixture. While decreasing the amount of DOPE to 30 mol% has no effect on the phase behavior in HBS, a further

decrease in the helper lipid content leads to the formation of a cubic phase; for SAINT-2/DOPE 80/20 (mol%), a cubic phase is observed in the temperature range explored.

2.4 MIXTURES OF SAINT-5 AND DOPE

2.4.1 Phase Behavior in Water: Rigidity of SAINT-5 Containing Lamellar Structures

Differential scanning calorimetric (DSC) measurements have been performed to investigate the influence of DOPE on the main phase transition temperature of SAINT-5, the surfactant with saturated tails (Figure 4).

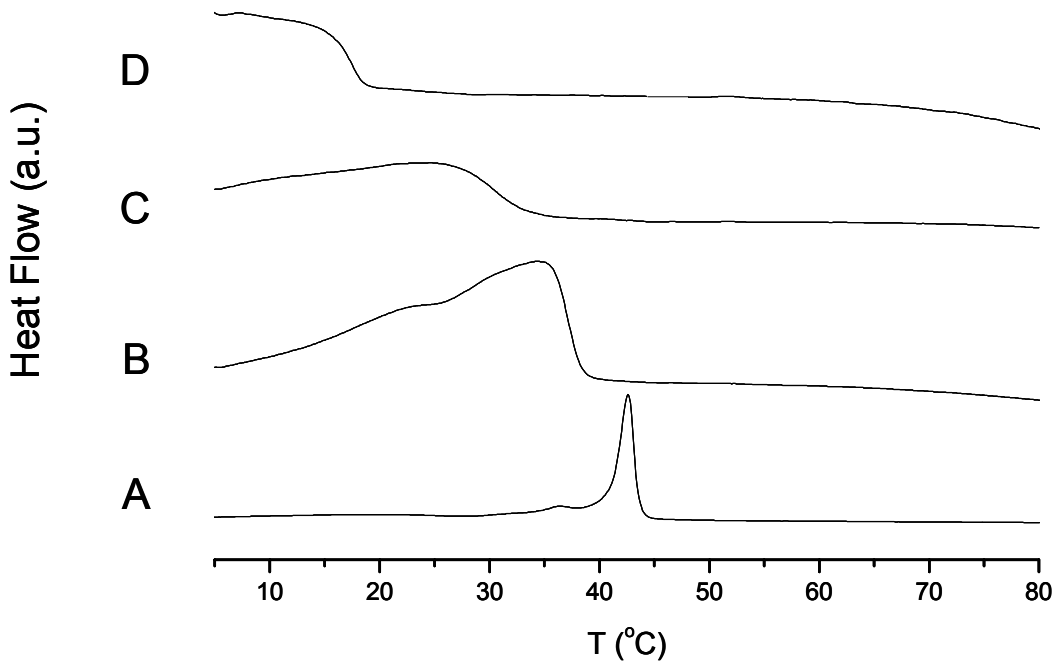

Figure 4 *DSC scans of SAINT-5/DOPE vesicles (5 mM total lipid concentration) in water: (A) 100/0, (B) 70/30, (C) 50/50, (D) 30/70 mol %.*

The temperature measured for the transition from the L_β to the L_α phase (T_m) is 43°C for pure SAINT-5, consistent with previous measurements.[5] Addition of DOPE decreases the T_m and broadens the coexistence region between the gel and the liquid-crystalline regions. While the transition to the liquid-crystalline phase for SAINT-5/DOPE 70/30 (mol%) is complete at 40°C, the equimolar mixture (optimal for transfection) is in the fluid state at 35°C (approximately the transfection temperature).

The ^{31}P-NMR spectra recorded on equimolar mixtures of SAINT-5/DOPE in water (Figure 5, top row) show that the lamellar organization is predominant in the region of the phase diagram under investigation and, in contrast with the surfactant with unsaturated chains, the isotropic signal is only clearly visible at 65°C.

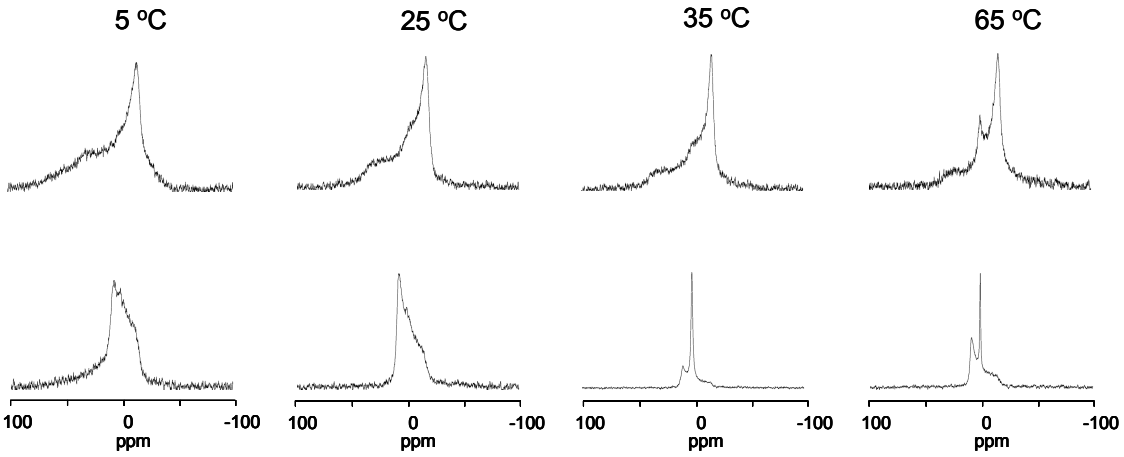

Figure 5 *^{31}P-NMR spectra as a function of increasing temperature of samples of SAINT-5 mixed with DOPE (1/1 mol. ratio, 100 mM total lipid concentration) in water (top row) and in HBS (bottom row).*

We can conclude that SAINT-5 and SAINT-2 in equimolar mixtures with DOPE exhibit similar morphologies in water: both phase diagrams are dominated by a lamellar organization. Nevertheless, while the equimolar mixture SAINT-2/DOPE is in the liquid-crystalline state at temperatures higher than 0°C (L_α phase), the main phase transition of the mixture with the saturated amphiphile SAINT-5 is complete only above room temperature (T > 30°C). These observations are consistent with the lower dynamic character of saturated alkyl chains with respect to unsaturated ones.[10] Compared to the L_α phase, the L_β phase gives rise to a broader ^{31}P-NMR signal with a less well-defined low field shoulder, due to the motional restriction of the phospholipids in the gel state. According to DSC data, the main phase transition of the equimolar mixture of SAINT-5 with DOPE is complete at 35°C, in agreement with the variations in the line shape in the ^{31}P-NMR spectra. The higher isotropic contribution to the line shape in the mixture of SAINT-2 compared to that of SAINT-5 provides further evidence for the higher fluidity of the mixtures containing the unsaturated amphiphile. Studies of the interaction of SAINT-5 monolayers with p-DNA, using ultra-pure water as the subphase,[1] showed that the recruitment of the lipid onto the lipoplex surface is hampered by the inability of the cationic surfactant to dissociate from the lipid monolayer.

The presence of the helper lipid DOPE leads only to a partial relief of this structural rigidity of the membrane and is insufficient to avoid deformation and decondensation of the DNA. This leads to inefficient DNA translocation which results in a poor transfection efficiency.[1] Our DCS and ^{31}P-NMR data are consistent with these suggestions; the only partial increase in fluidity of the equimolar mixture of SAINT-5/DOPE finds an explanation in the fact that when the complexation with DNA is carried out at room temperature, lipids are present in coexisting gel and liquid-crystalline phases.

2.4.2 Phase Behavior at Physiological Ionic Strength: Inhomogeneous Mixing with the Helper Lipid.

According to ^{31}P-NMR experiments (Figure 5, bottom row), the phase behavior of the mixture of SAINT-5 with DOPE appears to be more complex in HBS. At 5°C, the broad signal indicates the coexistence of L_β, H_{II} and cubic phases. Upon increasing the temperature to 25°C, the contribution of an H_{II} phase becomes predominant. At 35°C the line shape is determined by the superposition of an isotropic peak and a weak signal arising from an H_{II} phase. The contribution of the H_{II} signal increases again with a further increase in temperature. The reversibility of the high-temperature transitions has been established by decreasing the temperature to 35°C and studying the cooling behavior. When the temperature is decreased to 25°C (Figure 6, left column), the line shape is different from that obtained at the same temperature in the heating array, showing only an isotropic peak (and no features due to H_{II} phases).

At 5°C the spectrum presents a broad, badly resolved component and is still dominated by the isotropic peak; after 24 hours of equilibration at 5°C, the broad component evolves into the typical line shape for the lamellar phase. The ^{2}H-NMR spectra recorded in the cooling array, (Figure 6, right column), show the same phases as detected by ^{31}P-NMR, suggesting the presence of a perfectly mixed system.

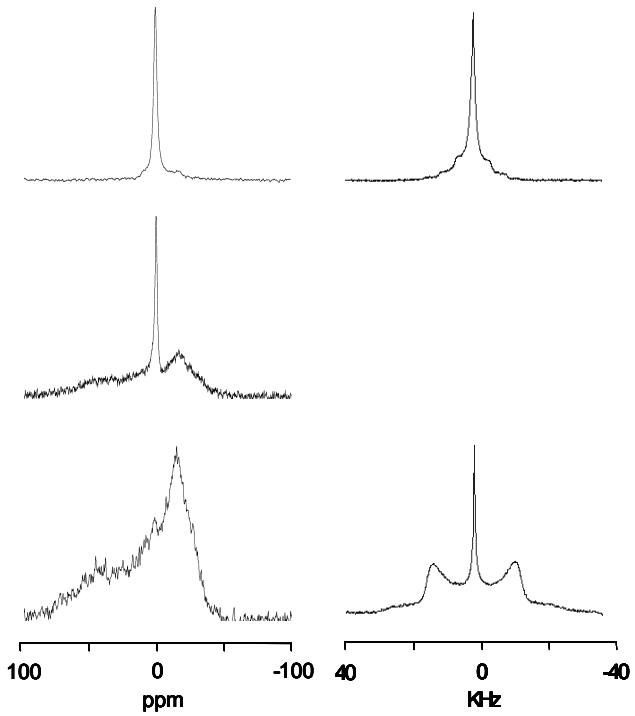

Figure 6 *^{31}P-NMR (left column) and ^{2}H-NMR (right column) spectra of SAINT-5 mixed with DOPE (1/1 mol. ratio) in HBS after equilibration of the sample at 65°C for one day. From top to bottom at 25°C, at 5°C after 30 minutes of equilibration and at 5°C after one day of equilibration.*

The analysis of the ^{2}H-NMR spectra recorded in the heating array (Figure 7) indicates that at 25°C the cationic amphiphile is mainly organized in a cubic phase (isotropic signal).

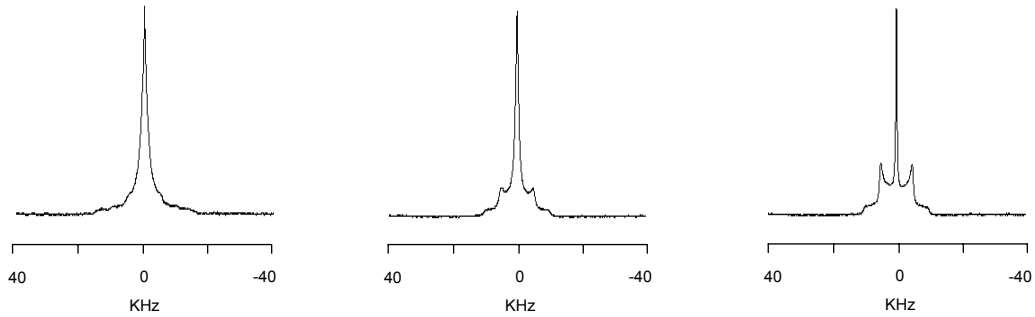

Figure 7 *^{2}H-NMR spectra of samples of SAINT-5 mixed with DOPE (1/1 mol. ratio, 100 mM total lipid concentration) in HBS. From left to right 25°C, 35°C, and 65°C.*

From the comparison with the ^{31}P-NMR spectra, we can conclude that the mixing of the cationic surfactant with the helper lipid is incomplete at room temperature and the H_{II} phase observed with ^{31}P-NMR at 25°C is due to domains of unmixed DOPE. Besides the reduction

of the cross-sectional headgroup area observed also for SAINT-2/DOPE mixtures, in the SAINT-5/DOPE system the salt-induced reduction of the electrostatic repulsion between the headgroups results into the demixing of the lipids.

From 35°C to 65°C, the correspondence between the ^{31}P-NMR and ^{2}H-NMR data indicates that the observed cubic and H_{II} phases are mixed lipid phases. Interestingly, in the cooling array, demixing is not observed after several hours at 5°C.

According to the regular solution model,[11] the enthalpic contribution (ΔH_m) to the Gibbs energy of mixing (ΔG_m) of the molecules *A* with the molecules *B*, depends on the effective interaction parameter, $\rho_0 \propto 2U_{AB} - U_{AA} - U_{BB}$, which relates to the difference in energy between unlike and like pair interactions. Negative values of ρ_0 favour mixing, resulting from unlike pair interactions stronger than the average interaction between like pairs. It follows that going from water to HBS the intermolecular repulsive interactions between SAINT-5 molecules are decreased to such an extent that domains of different lipid compositions are formed. Upon increasing the temperature, the favourable entropic contribution to the Gibbs energy of mixing is increased leading to $\Delta G_m < 0$ only above 25°C.

When the amphiphiles are mixed at 35°C, the H_{II} phase coexists with a dominating isotropic phase. A further increase in temperature increases the contribution of the H_{II} phase. The transition is consistent with an increase in *P*; at high(er) temperatures the cross-sectional headgroup area decreases as a consequence of the decrease in the hydration shell and the hydrophobic volume increases, due to the increased mobility of the alkyl chains. The coexistence of different phases in the same lipoplex preparation might occur when the phases have a similar Gibbs energy or if a high kinetic barrier for the transition is present. The reversibility of the observed transition, within short equilibration times, indicates that the coexisting phases have similar Gibbs energies and no significant kinetic barrier impedes the transition.

Decreasing the amount of DOPE leads to a smaller contribution to the line shape of the high temperature H_{II} phase with respect to the cubic phase; in SAINT-5/DOPE 90/10 (mol%), this mixed H_{II} phase is no longer detectable.

2.5 MIXTURES OF SAINT-5 WITH DOPS

When the lipoplex interacts with the cellular membrane, the composition of the lipoplex can vary as a consequence of the recruitment of membrane lipids; the exchange of lipids can have considerable effects on the morphology of the lipoplex, with important implications for

the transfection efficiency.[1] Major reasons may involve the translocation of the DNA across the cellular membrane and endosomal escape. It was found previously that lipoplexes of SAINT-5/DOPE can assume the H_{II} morphology after interaction with anionic vesicles.[1]

Experiments on mixtures of SAINT-2/DOPE/DOPS 2.5/2.5/1 (Figure 8) confirm the effect of the negatively-charged phospholipid. While at 5°C different phases are present, at temperatures above 25°C only the H_{II} phase is detectable. The spectra recorded for this sample in the cooling array showed complete reversibility of the transitions, in contrast with observations in the absence of the negatively-charged phospholipid (*vide supra*).

As previously shown by SAXS measurements,[1] pelleted SAINT-5/DOPE lipoplexes at a charge ratio +/- = 2.5 are unable to adopt an H_{II} phase in HBS at room temperature. Interestingly, incubation of SAINT-5/DOPE lipoplexes with vesicles containing anionic phospholipids leads to the formation of the H_{II} phase at room temperature.

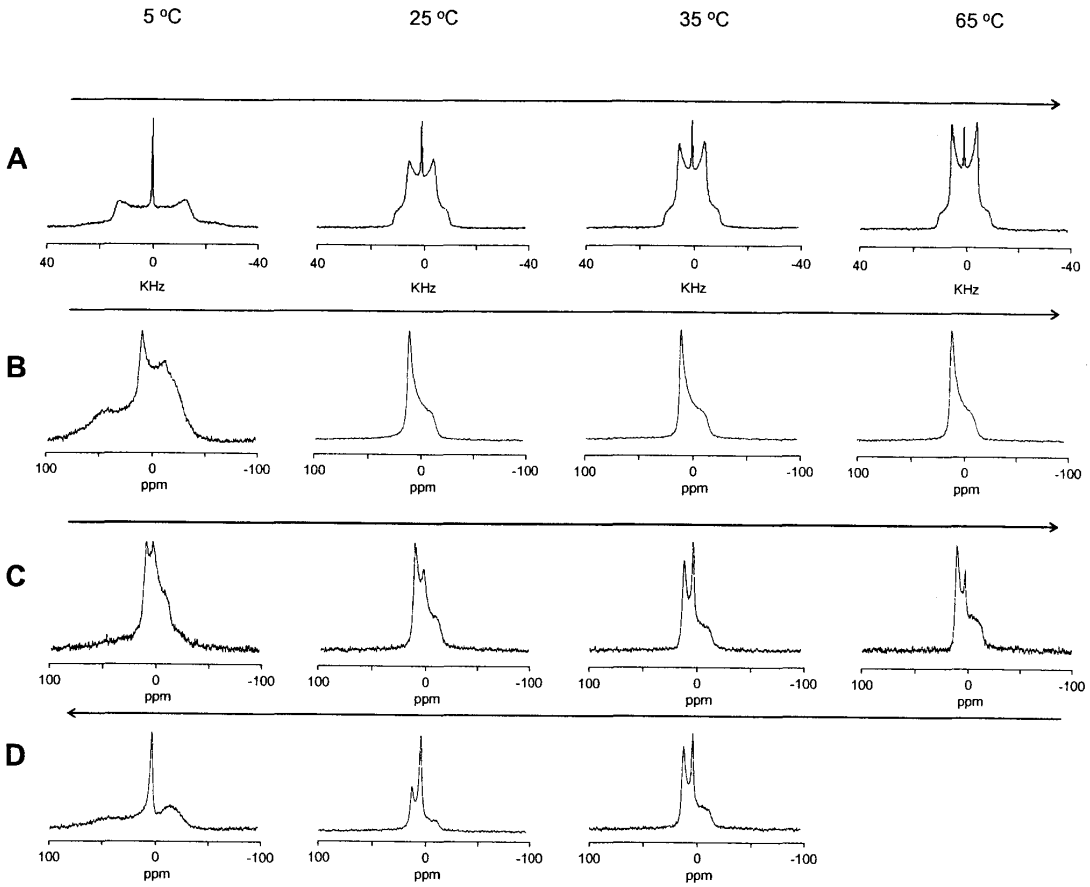

Figure 8 *^{2}H (A) and ^{31}P-NMR (B) spectra of SAINT-5/DOPE/DOPS 2.5/2.5/1 in HBS. Heating (C) and cooling (D) ^{31}P-NMR spectra array of SAINT-5/DOPE 2.5/3.5. The arrow above each spectra array indicates the direction of the temperature variation.*

The ^{2}H- and ^{31}P-NMR experiments shown in Figure 8A and B, respectively, clearly indicate that an amount of negatively charged phospholipid which introduces the same number of negative charges as the DNA at the optimal charge ratio for transfection, leads to the quantitative formation of an H_{II} phase at room temperature. The correspondence between the data obtained by monitoring the cationic amphiphile and the phospholipids independently using both ^{2}H- and ^{31}P-NMR, and the complete reversibility of the transitions observed within short equilibration times in the cooling array, are consistent with a good mixing of the components. To verify that the variation in the phase behavior observed after the introduction of DOPS is due to the presence of the negative charge in the headgroup region and not to the increased number of unsaturated alkyl chains, the experiments reported in Figure 8C and D have been performed. Replacing DOPS by the same amount of DOPE does not lead to a significant change with respect to the equimolar mixture SAINT-5/DOPE. The negatively charged phospholipid has therefore both the effect of increasing the packing parameter, favouring H_{II} phase formation, and of insuring the mixing of the lipids.

2.6 MORPHOLOGY OF THE SAINT-2/DOPE LIPOPLEX

The effect of plasmid DNA complexation on the morphology of SAINT-2/DOPE mixtures in water and in HBS has been investigated by monitoring the ^{31}P CSA and ^{2}H quadrupolar splittings of the lipoplexes. The ^{31}P-NMR spectra of the mixture in water (Figure 9) are dominated by an isotropic component in the complete temperature range explored (5-65 °C). At 5 °C the isotropic signal is superimposed on a bilayer component, with a line shape characteristic of a system in which the CSA is partially averaged.[12] Analogous ^{31}P-NMR line shapes were obtained for DOTMA/DOPE lipoplexes[3] but they were not assigned to a specific lipid structure. The phosphate groups of the DNA[3] give rise to a broad peak with a half-width of about 100 ppm, not clearly visible in these spectra, as expected on the basis of the ratio between lipid and DNA phosphate groups used.

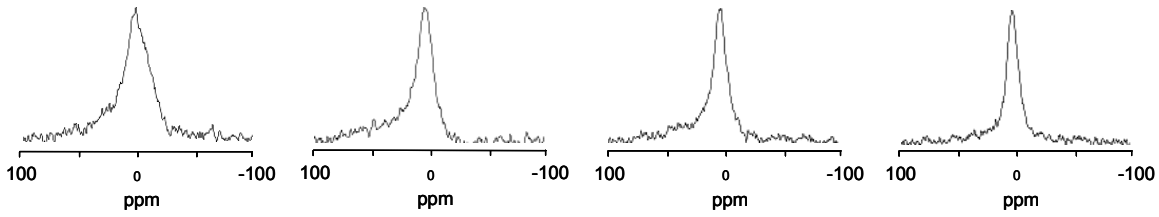

Figure 9 *^{31}P-NMR spectra of lipoplex formed from equimolar mixtures of SAINT-2/DOPE with plasmid DNA (+/- charge ratio 2.5) in water. From left to right, the temperature is 5, 25, 35 and 65°C.*

The ^{2}H-NMR spectrum (Figure 10, left) at 5°C shows an isotropic signal together with a broad component. Rising the temperature leads to narrowing of the broad component.

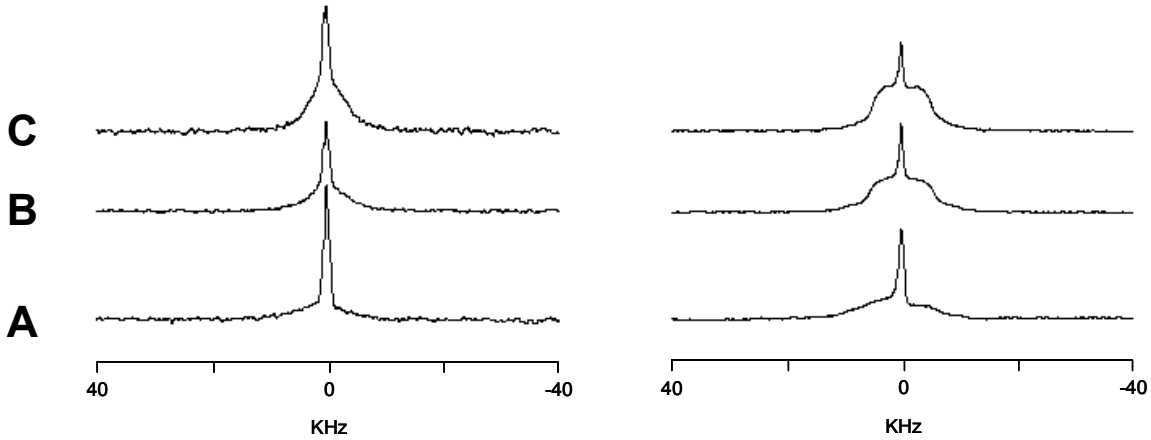

Figure 10 *^{2}H-NMR spectra of lipoplex of equimolar mixtures of SAINT-2-d3/DOPE with plasmid DNA (+/- charge ratio 2.5) in water (on the left) and HBS (on the right), at 5°C (A), 35°C (B) and 65°C (C).*

The ^{2}H-NMR line shapes indicate the presence of an anisotropic phase in which a mechanism of averaging of the quadrupolar interaction is active. This effect increases with temperature.

High-resolution cryo-TEM pictures have been recorded of the same sample (Figure 11), which provided new insights into the lipoplex morphology and helped rationalizing the NMR results.

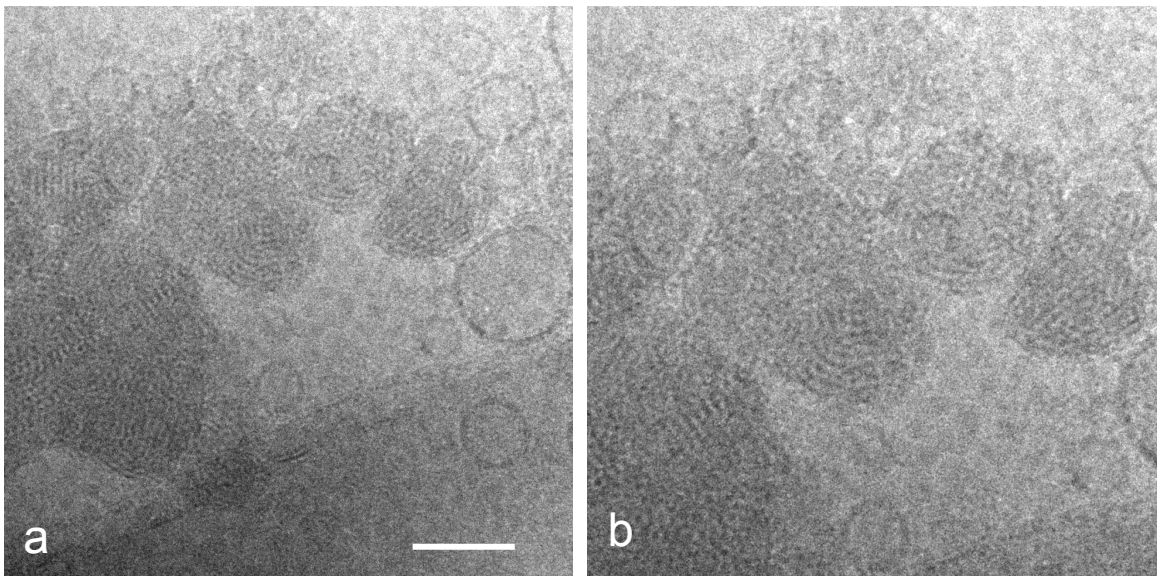

Figure 11 *Cryo-TEM picture of the lipoplex formed from equimolar mixtures of SAINT-2/DOPE and plasmid DNA (+/- charge ratio 2.5) (a). On the right, an expansion is shown to facilitate the visualization of the characteristic features (b). The bar represents 100 nm.*

It is evident from the cryo-TEM data that under conditions of such a large excess of positive relative to negative charges, part of the vesicle population remains unbound to the DNA. The tumbling in solution and the lateral diffusion of the lipids around the highly curved surfaces of these aggregates (diameters smaller than 100 nm) completely average out the anisotropy leading to the isotropic peak present also at low temperatures. Moreover, the results confirm the lamellar organization previously observed for the pelleted lipoplex.[8]

At the concentration used, the colloidal stability of the complexes is low and formation of macroscopic aggregates is observed after a short time (< 1 min). Besides the large size of the complexes, both ^{31}P and ^{2}H-NMR clearly showed that an effective mechanism of averaging of the anisotropy was active. The high quality of the cryo-TEM pictures clearly establishes the absence of extended lamellae in the complex. The bilayers are folded to form small diameter loops. This particular organization has been previously observed for different surfactants[13-15] and does not seem to depend on the type of DNA used for the lipoplex preparation.[15] The NMR experiments show that the anisotropic interactions are averaged to a large extent with the anisotropic contribution being observable only at 5°C, *i.e.* the reorientation of the molecules is fast on the NMR time scale. The cryo-TEM pictures help to rationalize the NMR results, since lateral diffusion around the small diameter loops is certainly an effective source of averaging of the CSA and of the quadrupolar interactions. Cryo-TEM pictures (Figure 12) also reveal that lipoplexes obtained at an excess of negative charge (+/- charge ratio 0.5) assume morphologies analogous to the complex at the optimal charge ratio for transfection and free vesicles are no longer present.

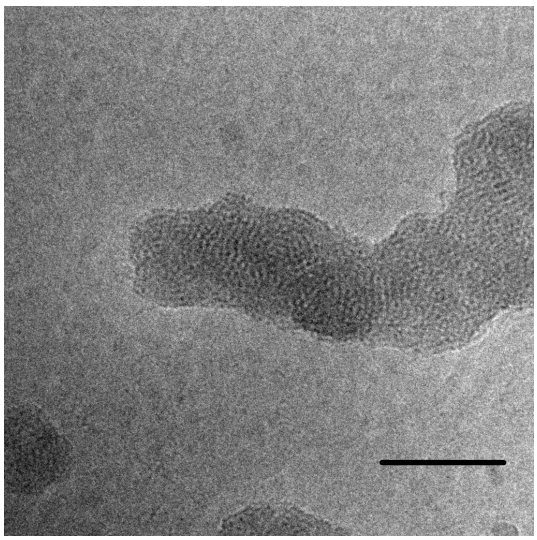

Figure 12 *Cryo-TEM picture of the lipoplex formed from equimolar mixtures of SAINT-2/DOPE and plasmid DNA (+/- charge ratio was 0.5). The bar represents 100 nm.*

The particular morphology observed in the lipoplex of SAINT-2 is not a unique feature of this amphiphile. Cryo-TEM pictures of lipoplexes of sugar-based gemini surfactants developed in our group[13] and of other transfection cocktails[14,15] show similar characteristics. In studies performed by Schmultz at al.,[16] the lipoplex morphology is also characterized by highly curved lamellae and a concentric "ring-like" pattern is recognizable. Some ring-like structures are easily identifiable in our system as well. It has been suggested that this particular morphology arises from cationic-liposome induced DNA compaction which appears to occur through a concentric winding, where DNA is adsorbed onto the cationic bilayers.[15] The characteristic pattern seems to be related to the structural changes, which DNA molecules undergo during DNA condensation. It has already been mentioned that analogous structures have been observed with plasmid DNA, linear DNA and with ODN (oligodeoxyribonucleotide).[15] Our results show that similar patterns, with bilayers folded in loops, are recognizable in lipoplexes formed by structurally different cationic amphiphiles. We contend that the observed morphology, characterized by highly curved bilayers, is the general aggregate organization for complexes between condensed nucleic acids and bilayer-forming cationic amphiphiles.

In HBS, at 5°C, a ^{2}H-NMR signal similar to the one in water was observed (Figure 10A, right column). Increasing the temperature leads to an irreversible transition to the H_{II} phase (Figure 10B, C, right column). The line shape of the ^{31}P-NMR spectra confirms the presence of the H_{II} phase. The measurements performed on the lipoplexes in HBS showed how the hexagonal morphology preferred by the equimolar SAINT-2/DOPE mixture in the absence of DNA remains the thermodynamically most stable phase also after interaction with the poly-anion.

2.7 CONCLUSIONS

We have performed an NMR-based investigation of the differences in phase behavior between the mixtures of two structurally related cationic amphiphiles, differing only in the degree of unsaturation of the alkyl chains, in combination with DOPE. The experiments were carried out under conditions relevant for gene transfection. The unsaturated surfactant SAINT-2 shows the highest dynamic character of the membranes formed. The different effects induced by an increase of the ionic strength to physiological values has been determined and rationalized on the basis of changes in the packing parameter. While the mixtures of the unsaturated surfactant (SAINT-2) form inverted phases and in particular

stable H_{II} phases for DOPE contents equal or higher than 30 mol%, the saturated surfactant (SAINT-5) does not form homogeneously mixed inverted phases in mixtures with DOPE at room temperature. However, mixed inverted phases are observed for this system at higher temperatures and, after mixing has been achieved by heating, metastable mixed phases are present for several hours also at 5°C. At 35°C the cubic phase is dominant.

The morphology of the lipoplex formed from an equimolar mixture of SAINT-2/DOPE and plasmid DNA is characterized by highly curved bilayers. We suggest that this organization is a general characteristic of complexes of bilayer-forming amphiphiles with DNA present in the condensed form, irrespective of the nature of the headgroup of the amphiphile.

Finally it has been established that the H_{II} morphology of the SAINT-2/DOPE lipoplex under physiological ionic strength conditions is thermodynamically stable.

Our results demonstrate the power and convenience of the combination of ^{2}H and ^{31}P-NMR experiments in studies of complex lipid/phospholipid mixtures, in particular when multiple phases coexist in the same preparation.

2.8 MATERIALS AND METHODS

Methyl iodide-d_3 was purchased from Deutero GmbH, Kastellaun, Germany, DEAE Sephadex A-25 from Amersham Pharmacia Biotech AB, Amersham, UK, 1,2-dioleoyl-*sn*-glycero-3-phosphoethanolamine (DOPE) and 1,2-dioleoyl-*sn*-glycero -3-[phospho-L-serine] (DOPS) from Avanti Polar Lipids Inc. (Alabaster, AL). All other chemicals were of analytical grade or purified according to standard procedures.[17]

N-Methyl{d_3}-4-(dioleyl)methylpyridinium chloride (SAINT-2 d_3)

^{1}H NMR (200 MHz): δ 9.47 (d, $^{3}J_{AB}$ = 6.4 Hz, 2 H, CH_{ar}), 7.72 (d, $^{3}J_{AB}$ = 6.4 Hz, 2 H, CH_{ar}), 5.33 (m, 4H, CH), 2.77 (m, 1H, CH), 2.00 (m, 8H, $CH_2CH{=}CHCH_2$), 1.75 (m, 4H, $CH(CH_2)_2$), 1.55 (m, 4H, CH_2CH_3), 1.25 (m, 44 H, CH_2), 0.87 (t, ^{3}J = 6.5 Hz, 6H, CH_3)

^{13}C-NMR (50.28 MHz): δ 167.1, 145.0, 130.3, 130.1, 129.8, 129.5, 126.8, 46.4, 35.5, 31.7, 29.5, 29.4, 29.3, 29.l, 29.0, 28.9, 27.2, 27.0, 22.4, 13.9.

N-Methyl{d_3}-4-(distearyl)methylpyridinium chloride (SAINT-5 d_3)

^{1}H NMR (200 MHz): δ 9.38 (d, $^3J_{AB}$ = 6.5 Hz, 2 H, CH_{ar}), 7.72 (d, $^3J_{AB}$ = 6.3 Hz, 2 H, CH_{ar}), 2.77 (m, 1H, CH), 1.48-1.78 (m, 4H, CH(CH_2)$_2$), 1.24 (m, 64H, CH_2), 0.87 (t, ^3J = 6.5 Hz, 6H, CH_3).

^{13}C-NMR (50.28 MHz): δ 167.1, 144.9, 126.8, 46.4, 35.4, 31.6, 29.4, 29.3, 29.1, 27.1, 22.4, 13.8.

Sample preparation

A sample of 7.1-kilobase DNA was isolated from Escherichia Coli using the Sigma-Aldrich GenElute HP Maxiprep kit (Sigma-Aldrich, Zwijndrecht, The Netherlands). The plasmid concentration was determined spectrophotometrically by measuring the absorption at 260 nm using the relation 1.0 A = 50 µg/ml. Typically, the A_{260}/A_{280} values were about 1.85.

A solution of the respective SAINT and the desired amount of DOPE in dichloromethane was dried under a stream of nitrogen and, hereafter, residual solvent was removed under high vacuum. For the study of the lipid phase behavior in the absence of DNA, the films were hydrated with bi-distilled water or HBS buffer (HEPES 15 mM, 150 mM NaCl, pH = 7.4) to a total lipid concentration of 0.1 M. The lipids were then vortexed and freeze-thawed five times to ensure homogeneous mixing.

To obtain small unilamellar vesicles, the lipid films were hydrated to a final total lipid concentration of 5 mM (unless stated otherwise) and, after vigorous vortexing, the suspension was tip-sonicated for 2 min (Branson Sonifier B15-P, Danbury, CT).

Lipoplexes in water were prepared by addition of the plasmid DNA to a vesicular suspension, reaching a final charge ratio (+ / -) equal to 2.5.

NMR-spectroscopy

^{31}P-NMR Spectroscopy: ^{31}P-NMR spectra were recorded on a Varian Unity-Plus 500 (Varian, Palo Alto, CA) operating at 202.653 MHz for the phosphorous channel. Data were acquired with single-pulse excitation under high power broadband proton decoupling. The 90° pulse length was 28 µs, the recycle delay 1.3 s, the spectral width 40.588 KHz and the data size 16.384. Typically, 4000 transients were signal-averaged and exponentially multiplied with a 50 or 100 Hz line broadening function before Fourier transformation. Spectra were measured at different temperatures, and samples were allowed to equilibrate at each temperature for at least 30 min before data collection.

^{2}H-NMR Spectroscopy: ^{2}H-NMR experiments were recorded on a Bruker Avance 500 WB (Bruker BioSpin Corp., Billerica, MA) NMR spectrometer (operating frequency 76.8 MHz), using a quadrupolar echo technique [18]. The recycling delay was 200 ms, echo delay was 30 μs, the 90° pulse was 6.15 μs, the spectral width 500 KHz and 20000–50000 scans were collected. Typically, before Fourier transformation, an exponential multiplication with a line-broadening factor of 100 Hz was used. Spectra were measured at different temperatures, and samples were allowed to equilibrate at each temperature for at least 30 min before data collection.

Differential Scanning Calorimetry

DSC scans on SUVs were taken on a NANO II – DSC (Calorimetry Sciences Corp., Lindon, UT) with a scan rate of 1°C/s. Eight heating scans were performed between 1 and 90°C. against a reference cell filled with water. The samples were allowed to equilibrate for 30 min. at 1°C between successive scans.

Cryo-Transmission Electron Microscopy

A drop of the lipid suspension was deposited on a glow discharged holey carbon-coated grid. After blotting away the excess of lipid, the grids were plunged in liquid ethane. The frozen specimen were mounted in a Gatan (model 626) cryo-stage and examined in a Philips CM 120 cryo-electron microscope (Philips, Eindhoven, Nederland) operating at 120 KV. Micrographs were taken under low dose conditions.

Small Angle X-Ray Scattering

SAXS measurements were performed at 25 °C on a NanoStar device (Bruker AXS and Anton Paar) with a ceramic fine-focus tube operated in a point focus mode. The tube was powered with a Kristalloflex K760 generator at 35 KV and 40 mA. The primary beam was collimated using cross-coupled Göbel mirrors and a 0.1 mm pinehole, providing a CuK_α radiation beam with a wavelength of 0.154 nm and a full-width at half maximum about 0.2 mm in diameter at the sample position. A sample-detector distance of 0.24 m was used. The use of a Hi-Star position-sensitive area detector (Siemens AXS) allowed the recording of the scattering intensity in the q range of 0.5-8.5 nm. The scattering vector q is defined as $q = (4\pi/\lambda)\sin(\theta/2)$ where λ is the wavelength and θ is the scattering angle. The measuring time was between 3 and 9 h.

2.9 APPENDIX 1: SAINT-2 CUBIC PHASES IN ^2H_2O

In order to get deeper insights into the aggregation properties of SAINT-2, the behavior of the binary cationic lipid/^2H_2O system has been investigated by ^{2}H-NMR, SAXS and cryo-TEM in a range of concentrations not immediately relevant for gene therapy applications.

Even if the cubic regions of lipid phase diagrams are often very narrow, the phase diagram of SAINT-2/^2H_2O is dominated by cubic phases in the whole composition range explored, *i.e.* ^2H_2O content from 50 to 80 in wt%. The biological and technological relevance of cubic phases has already been discussed in Paragraph 1.2.3.1. A particularly interesting feature of the phase diagram of SAINT-2 in water, which emerged from this study, is the presence of a cubic phase in equilibrium with water, a characteristic displayed by only few surfactants.

2.9.1 ^{2}H-NMR

^{2}H-NMR experiments have been performed on samples of SAINT-2 hydrated with increasing amounts of ^2H_2O. A representative spectrum is reported in Figure A1. 1.

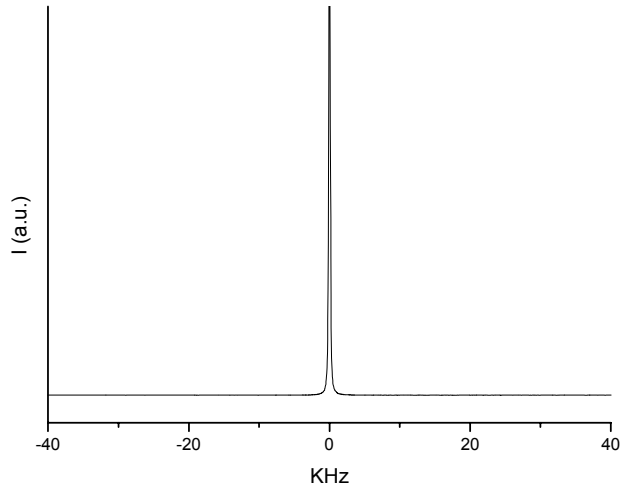

Figure A1. 1 *^{2}H-NMR spectrum of SAINT-2/D_2O 50/50 wt%. The spectra recorded for water contents up to 80 mol% show an analogous isotropic peak.*

In the range of compositions explored, all the spectra exhibit only a sharp isotropic peak (the line widths at half-height of the signals for the samples containing 50, 60, 70 and 80 wt% of ^2H_2O are 225, 245, 235 and 173 Hz, respectively). The motional averaging of the quadrupolar interaction of ^2H_2O is an indication of the presence of isotropic phases, as lateral diffusion of the hydrated lipids results in averaging of the anisotropy over all orientations. Although an isotropic contribution to the line shape could arise from bulk water, all the

samples under investigation appeared to be very viscous and only for the highest water contents excess water was clearly visible.

2.9.2 SAXS measurements

The isotropic phases identified by ^{2}H-NMR have been further characterized by SAXS. Table A1. 1 features the X-ray scattering data of these samples.

Table A1. 1 *Summary of the SAXS results for SAINT-2 in D_2O.*

Pn3m		**Im3m**			
	S-2 50 wt%		S-2 40 wt%	S-2 30 wt%	S-2 20 wt%
(h, k, l)	q(Å^{-1})	(h, k, l)	q(Å^{-1})	q(Å^{-1})	q(Å^{-1})
(1 1 0)	0.091	(1 1 0)	0.060	0.059	0.057
(1 1 1)	0.112	(2 0 0)	0.084	0.084	0.081
(2 0 0)	0.129	(2 1 1)	0.102	0.102	0.099
(2 1 1)	0.159	(2 2 0)	Not shown	Not shown	Not shown
(2 2 0)	0.183	(3 1 0)	Not shown	Not shown	Not shown
(2 2 1)	0.193	(2 2 2)	0.144	Not shown	Not shown
		(3 2 1)	0.156	0.155	0.150
		(4 0 0)	Not shown	Not shown	Not shown
		(4 1 1) (3 0 0)	Not shown	0.175	Not shown
	a = 97.4		a = 152.6	a = 153.4	a = 157.5

Two representative spectra are reported in Figure A1. 2. Figure A1. 2A shows the diffraction pattern recorded on the mixture SAINT-2/^2H_2O = 50/50 in wt%. Several reflections are observed which can be indexed to a cubic phase of the primitive *Pn3m* space group on the base of their relative positions $(1,\ \sqrt{3/2},\ \sqrt{2},\ \sqrt{3},\ 2,\ 3/\sqrt{2})$**.** As

presented in the insert, the plot of the inverse spacing (1/d, Å^{-1}) against $\sqrt{h^2+k^2+l^2}$, where h, k, l are the Bragg parameters, is a straight line passing through the origin, which supports the reliability of the tentative assignment.

The unit cell length calculated from the line slope is 9.7 nm. Analogous treatment of the data for the samples with higher water content (Table A1. 1) shows a transition toward a cubic phase with different symmetry. The space ratios (1, $\sqrt{2}$, $\sqrt{3}$, 2, $\sqrt{5}$, $\sqrt{6}$, $\sqrt{7}$, $2\sqrt{2}$, 3) of the samples in which the amount of ^2H_2O is increased up to 80 wt% (Figure A1. 2) are all consistent with the Im3m space group.

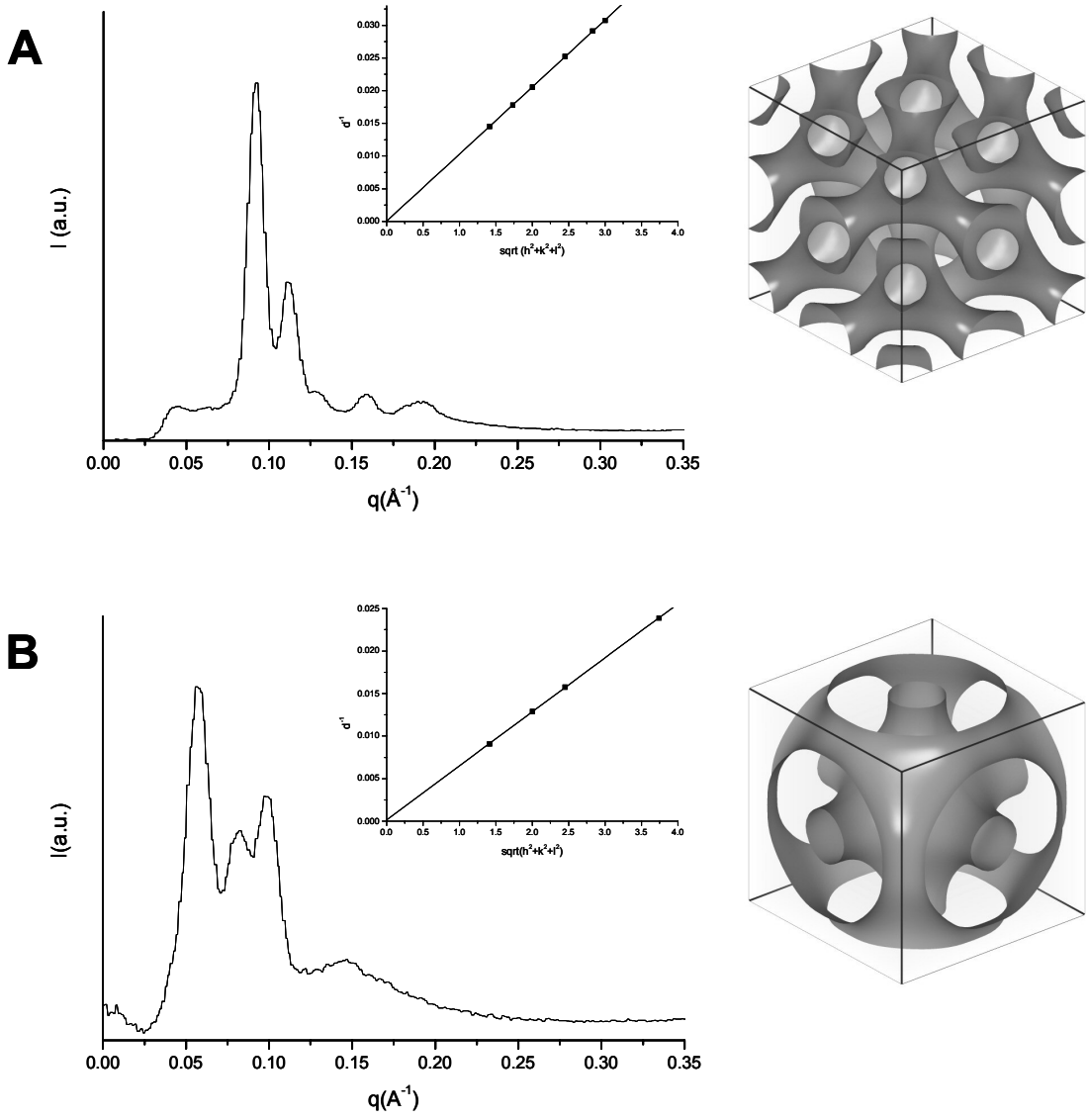

Figure A1. 2 *SAXS spectrum obtained on a SAINT-2/^2H_2O 50/50 wt% (A) and 20/80 wt% (B) dispersions; in the inserts, plots of the inverse spacing $1/d$ against $\sqrt{h^2+k^2+l^2}$ and models of the assigned cubic structures (Pn3m and Im3m, respectively) are shown.*

2.9.3 Cryo-TEM

The aggregates formed by the sample SAINT-2/^2H_2O 20-80 in wt% have been studied by cryo-TEM (Figure A1. 3).

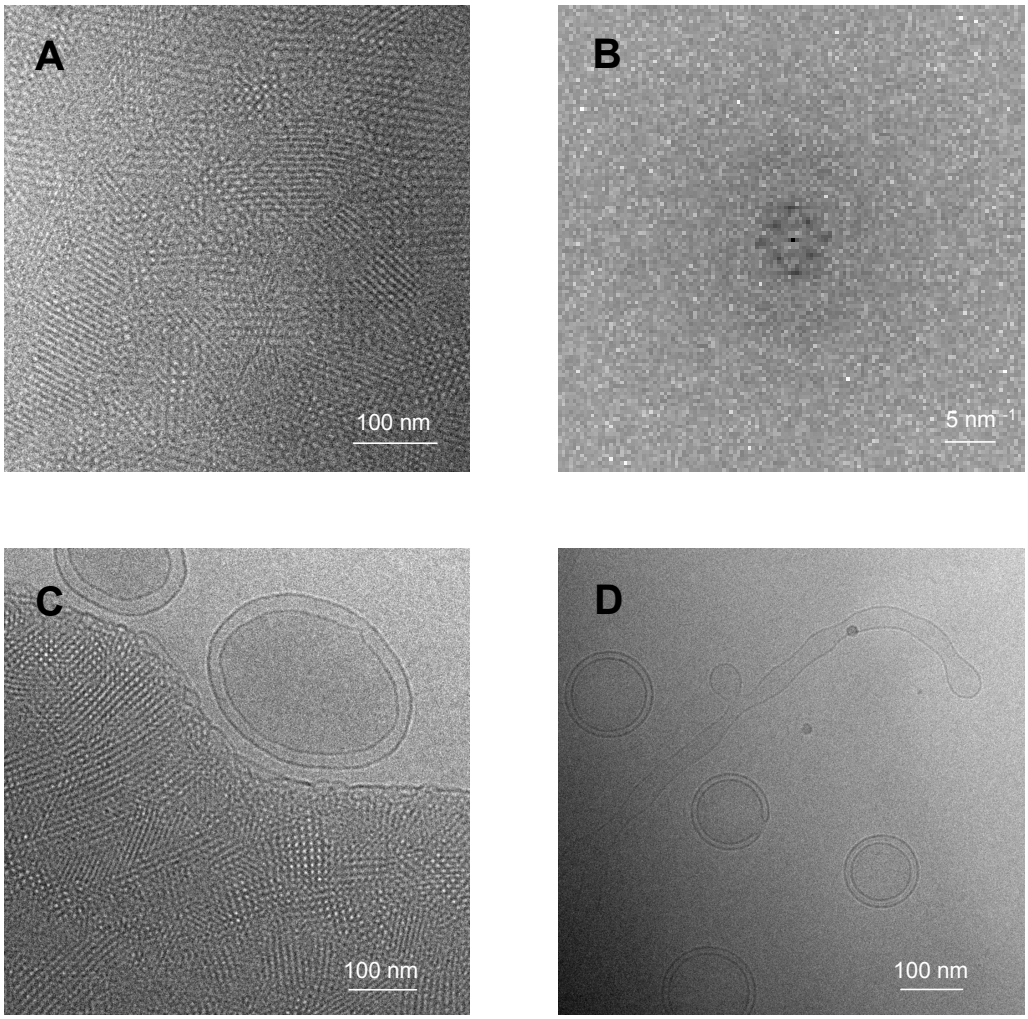

Figure A1. 3 *Cryo-TEM pictures of SAINT-2/^2H_2O 20/80 (A, B, D). In (B), the Fourier transform of an homogeneous part of (A) is shown.*

From the appearance of the texture, it is evident that the aggregates have a cubic liquid crystalline structure. It is also evident that the overall structure is characterized by different textures arising from cubic crystals oriented in different directions. The Fourier Transform of a section of the cryo-TEM picture in which the texture appeared constant is presented in Figure A1. 3B. The derived repeated distances are 57 Å and 114 Å. From the SAXS data, we derived a unit cell length of 157.5 nm. The corresponding separation between the (1 1 0) and (2 2 0) is respectively $157.5/\sqrt{2} = 111.5$ Å and $157.5/\left(2\sqrt{2}\right) = 55.7$ Å, in good agreement with

the values obtained from the micrographs. In the outermost surface region, lamellar features are visible (Figure A1. 3C). A minor population of vesicles has also been observed (Figure A1. 3C, D) together with extended tubular structures. Metastable vesicular aggregates are often present in lipid suspensions and they do not imply coexistence of lamellar and cubic phases.[19]

2.9.4 Concluding Remarks: SAINT-2 Cubic Phases as Drug Delivery Vehicles?

Even if this study had not been not carried out under rigorously controlled experimental conditions, especially as far as the exact water content of the lipid preparations is concerned, the results provide insights into some interesting characteristics of the phase behavior of SAINT-2. Hydration of this amphiphile leads to the formation of cubic phases in a broad range of compositions. Cubic phases with different symmetries are formed at different water contents and a transition form a cubic phase of the *Pn3m* space group to one of the *Im3m* space group is observed upon increasing the water content from 50 to 60 wt%. For water contents up to 80 wt%, the symmetry of the cubic phases does not change and the unit cell length slightly increases for increasing water contents. Cubic phases have been used as drug delivery vehicles and the lipid which is most commonly used for this purpose is monoolein,[20,21] a metabolite of fat digestion in the upper intestine. The phase diagram of monoolein as a function of the water content shows a transition from a *Ia3d* cubic phase to a *Pn3m* cubic phase which is stable even in the presence of excess water.[22] Cubic phases corresponding to the space group *Im3m* have been described in monoolein-poloxamer 407 (block copolymer: polyethylene oxide-polypropylene oxide-polyethylene oxide)-water[23] or monoolein-NMP (N-methylpyrolidinone)-water[24] systems. The analogies in phase behavior between monoolein- and SAINT-2-containing systems, and in particular a cubic phase stable in the presence of excess water, suggest the possibility for a more general use of SAINT-2 for drug delivery applications. The parenteral administration of drugs incorporated into cubic phases is limited by the high viscosity of these aggregates, which makes them difficult to inject, and by their general incompatibility with the intravenous route.[21] It follows that the colloidal stability of the dispersed cubic phase (cubosomes®)[25] is a fundamental issue and several studies of the preparation and stabilization of cubosoms have been conducted.[23,26-29] The possibility of stabilizing sub-micron cubic particles of SAINT-2 by adding pegylated SAINT derivatives[30] should be explored, in view of the possible application in the field of controlled drug delivery.

2.10 ACKNOWLEDGMENTS

Prof. Antoinette Killian (University of Utrecht, The Netherlands) and her group (in particular dr. Vladimir Chupin) are kindly acknowledged for their precious help with the ^{31}P- and ^{2}H-NMR measurements. I thank Dr. Markus Johnsson (Camurus AB, Lund, Sweden) for inspiring discussion, in particular about the cubic phases of SAINT-2 in water.

2.11 REFERENCES

1. Zuhorn, I. S.; Oberle, V.; Visser, W. H.; Engberts, J. B. F. N.; Bakowsky, U.; Polushkin, E.; Hoekstra, D. *Biophys. J.* **2002,** *83*, 2096-2108.

2. Mitrakos, P.; Macdonald, P. M. *Biochemistry* **1996,** *35*, 16714-16722.

3. Monk, K. W. C.; Cullis, P. R. *Biophys. J.* **1997,** *73*, 2534-2545.

4. Van der Woude, I.; Wagenaar, A.; Meekel, A. A. P.; Ter Beest, M. B. A.; Ruiters, M. H. J.; Engberts, J. B. F. N.; Hoekstra, D. *Proc. Natl. Acad. Sci. USA* **1997,** *94*, 1160-1165.

5. Meekel, A. A. P.; Wagenaar, A.; Šmisterová, J.; Kroeze, J. E.; Haadsma, P.; Bosgraaf, B.; Stuart, M. C. A.; Brisson, A.; Ruiters, M. H. J.; Hoekstra, D.; Engberts, J. B. F. N. *Eur. J. Org. Chem.* **2000,** *4*, 665-673.

6. Cullis, P. R.; De Kruyff, B. *Biochim. Biophys. Acta* **1979,** *559*, 399-420.

7. Scherer, P. G.; Seelig, J. *Biochemistry* **1989,** *28*, 7720-7728.

8. Šmisterová, J.; Wagenaar, A.; Stuart, M. C. A.; Polushkin, E.; ten Brinke, G.; Hulst, R.; Engberts, J. B. F. N.; Hoekstra, D. *J. Biol. Chem.* **2001,** *276*, 47615-47622.

9. Leigh, I. D.; McDonald, M. P.; Raymond, M. W.; Tiddy, G. J. T.; Tuzi, S. *J. Chem. Soc. ,Faraday Trans. 1* **1981,** *77*, 2867-2876.

10. Iwahashi, M.; Kasahara, Y.; Matsuzawa, H.; Yagi, K.; Nomura, K.; Terauchi, H.; Ozaki, Y.; Suzuki, M. *J. Phys. Chem. B* **2000,** *104*, 6186-6194.

11. Lee, A. G. *Biochim. Biophys. Acta* **1977,** *472*, 285-344.

12. Gorenstein, D. G. *Phosphorus-31 NMR;* Academic Press, INC.: **1984**.

13. Bell, P. C.; Bergsma, M.; Dolbnya, I. P.; Bras, W.; Stuart, M. C. A.; Rowan, A. E.; Feiters, M. C.; Engberts, J. B. F. N. *J. Am. Chem. Soc.* **2003,** *125*, 1551-1558.

14. Lasic, D. D.; Strey, H.; Stuart, M. C. A.; Podgornik, R.; Frederik, P. M. *J. Am. Chem. Soc.* **1997,** *119*, 832-833.

15. Schmutz, M.; Durand, D.; Debin, A.; Palvadeau, Y.; Etienne, A.; Thierry, A. R. *Proc. Natl. Acad. Sci. USA* **1999,** *96*, 12293-12298.

16. Schmutz, M.; Durand, D.; Debin, A.; Palvadeau, Y.; Etienne, A.; Thierry, A. R. *Proc. Natl. Acad. Sci. USA* **1999,** *96*, 12293-12298.

17. Vogel, A. I. *A Text-Book of Practical Organic Chemistry;* Third ed.; Longmans: London, **1962**.

18. Davis, J. H.; Jeffrey, K. R.; Bloom, M.; Valic, M. I.; Higgs, T. P. *Chem. Phys. Lett.* **1976,** *42*, 390-394.

19. Gustafsson, J.; LjusbergWahren, H.; Almegren, M.; Larsson, K. *Langmuir* **1996,** *12*, 4611-4613.

20. Engström, S. *Lipid Technol.* **1990,** *2*, 42-45.

21. Shah, J. C.; Sadhale, Y.; Chilukuri, D. M. *Adv. Drug Del. Rev.* **2001,** *47*, 229-250.

22. Hyde, S. T.; Andersson, S.; Ericsson, B.; Larsson, K. *Zeit. fur Krist.* **1984,** *168*, 213-219.

23. Landh, T. *J. Phys. Chem.* **1994,** *98*, 8453-8467.

24. Imberg, A.; Evertsson, H.; Stilbs, P.; Kriechbaum, M.; Engstrom, S. *J. Phys. Chem. B* **2003,** *107*, 2311-2318.

25. Andersson, S.; Jacob, M.; Lidin, S.; Larsson, K. *Zeit. für Krist.* **1995,** *210*, 315-318.

26. Siekmann, B.; Bunjes, H.; Koch, M. M. H.; Westesen, K. *Int. J. Pharm.* **2002,** *244*, 33-43.

27. Gustafsson, J.; Ljusberg-Wahren, H.; Almegren, M.; Larsson, K. *Langmuir* **1997,** *13*, 6964-6971.

28. Monduzzi, M.; Ljusberg-Wahren, H.; Larsson, K. R. *Langmuir* **2000,** *16*, 7355-7358.

29. Nakano, M.; Sugita, A.; Matsuoka, H.; Handa, T. *Langmuir* **2001,** *17*, 3917-3922.

30. Rejman, J.; Wagenaar, A.; Engberts, J. B. F. N.; Hoekstra, D. *Biochim. Biophys. Acta* **2004,** *1660*, 41-52.